A Simple All-in-One Shared-Aperture Decoupling Network (SADN) for Coupling Management in A Tri-Band Differentially-Fed Antenna (DFA) Array

Xichen Wang[(1)], Can Ding[(2)], Shiyong Li[(1),(3)], Guoqiang Zhao[(1),(3)], Houjun Sun[(1),(3)]

(1) The Beijing Key Laboratory of Millimeter Wave and Terahertz Technology, Beijing Institute of Technology (BIT), Beijing, China (wangxichen000512@163.com)

(2) The Global Big Data Technologies Center, University of Technology Sydney (UTS), NSW, Australia

(3) The Tangshan Research Institute, Beijing Institute of Technology (BIT), Tangshan, China (lishiyong@bit.edu.cn)

***Abstract*—A shared-aperture decoupling network (SADN) is developed to mitigate multiple types of mutual couplings within a tri-band antenna array, comprising two high-band (HB), two middle-band (MB) and two low-band (LB) differentially-fed antennas (DFAs). The SADN is an all-in-one decoupling solution but features remarkable simplicity and compact size. A decoupled tri-band DFA array operating in the LB (9.8–10.2 GHz, 3.5%), MB (18.1–19.2 GHz, 6.1%), and HB (25.5–28.9 GHz, 12.5%) has been designed, fabricated, and experimentally validated. The results demonstrate impressive in-band isolation levels of 28 dB, 27 dB, and a remarkable 52 dB at the center frequencies of LB, MB, and HB. Additionally, cross-band coupling is also effectively suppressed. All isolations between any two ports of the six antennas across the three bands are maintained larger than 20 dB. This superior decoupling performance is achieved through the novel symmetrical residual current cancellation (SRCC) principle, specifically designed for and uniquely applicable to DFAs.**

I. INTRODUCTION

The advancement of wireless communication technologies has precipitated an explosion in the number of devices and systems that necessitate concurrent operation across various frequency bands. Consequently, the multi-band shared-aperture antenna array has emerged to comply this burgeoning demand trend. However, when multi-band antennas are tightly arranged in close proximity, the interference between elements, including in- and cross-band coupling, severely compromises the array performance [1]. Effective antenna decoupling techniques become imperative to ensure optimal system operation.

Most of the available decoupling methods are designed for single-band antennas, but their application to multi-band arrays presents a new set of challenges, as both in-band and cross-band couplings must be addressed simultaneously across multiple bands. The design of multi-band shared-aperture antennas inherently involves managing couplings among different antennas to some extent. However, existing approaches typically employ separate decoupling structures for each type of coupling, which are then integrated [1]-[3]. Accommodating individual decoupling structures for each band increases the system size, profile, and complexity of multi-band antenna arrays, representing the first problem addressed in this work.

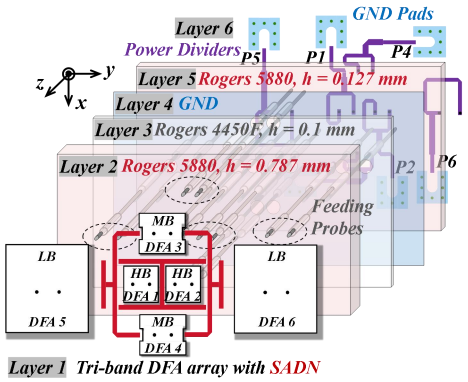

Figure 1. Schematic diagram of the tri-band DFA array with the shared-aperture decoupling network (SADN).

Meanwhile, differentially-fed antenna (DFA) has become a research hotspot due to its advantages of high anti-interference and low cross-polarization brought by its symmetrical structure [4]-[5], and its application in multi-band antenna array can further improve the performance. There have been some recent decoupling works specifically for DFAs that can achieve decoupling while maintaining symmetry, but all have narrow bandwidth. For example, the decoupling bandwidth reported in [4] and [5] are only 0.6% and 2.9%, respectively. Improving the decoupling bandwidth for closely spaced DFAs represents the second problem to be addressed in this work.

In this work, the two aforementioned problems are addressed using an all-in-one decoupling solution, the shared-aperture decoupling network (SADN). This simple yet effective network is based on a novel decoupling principle called symmetrical residual current cancellation (SRCC), specifically designed for and applicable only to DFAs. Unlike existing decoupling methods that aim to minimize the induced currents on the coupled antenna, the SRCC approach allows for residual currents but ensures they are identical at the two differential ports, canceling each other due to differential feeding. This relaxed restriction simplifies the decoupling structure and significantly broadens the decoupling bandwidth.

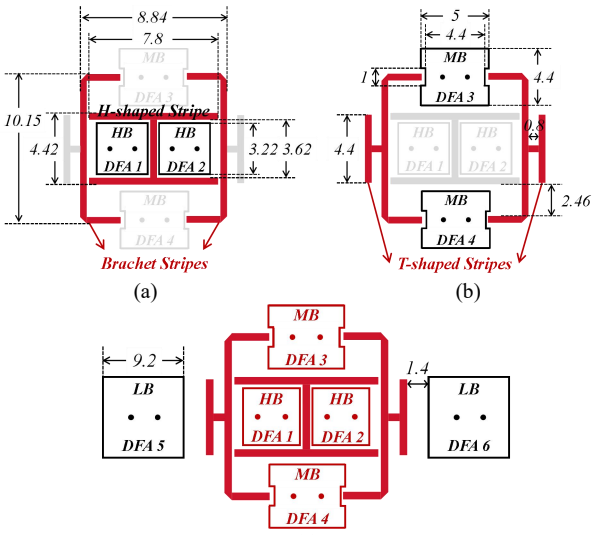

Figure 2. Effective components of the SADN for improving isolations in (a) HB, (b) MB, and (c) LB.

As shown in Fig. 1, a compact tri-band DFA array is proposed, with decoupling achieved through the SADN, represented by the red strip lines. The array comprises three pairs of differentially-fed patches on the top layer, each operating in distinct frequency bands: LB (9.8–10.2 GHz, 3.5%), MB (18.1–19.2 GHz, 6.1%), and HB (25.5–28.9 GHz, 12.5%), with a frequency ratio of 1:1.85:2.8. With this simple configuration and extremely close edge-to-edge distances between the patches, the array achieves in-band isolations of better than 28 dB, 27 dB, and 20 dB for the LB, MB, and HB bands, respectively, and cross-band isolations exceeding 22 dB. Positioned on the same layer as the patches, the SADN effectively addresses both in-band couplings (among the LB, MB, and HB antennas) and cross-band couplings (between antennas operating at different bands).

II. Decoupling Principle of the SADN

Fig. 1 presents an exploded view of the tri-band array, comprising three substrate layers and three metal layers. From top to bottom: The first layer is a metal layer, accommodating the six patches and the SADN on a single layer. The second layer is the main substrate layer supporting the patch antennas. The third layer is a thin prepreg layer, followed by the ground plane as the fourth layer. Below the ground plane is another substrate layer, which holds the feed lines for the array. Six differential power dividers are printed on the bottom layer to feed the six patches differentially. Feeding probes traverse all layers to connect the patches on the top layer with the feed networks located on the bottom layer. Despite having six layers, the total profile of the array is only 1.014 mm, corresponding to 0.03 wavelengths at the center frequency of the LB (10 GHz).

To illustrate the aperture sharing essence of the SADN, Figs. 2(a) to 2(c) highlight the components of the SADN that contribute to the improvement of isolation at the HB, MB, and LB, respectively. The SADN employs distinct working mechanisms to address different types of couplings, which will be discussed in detail below.

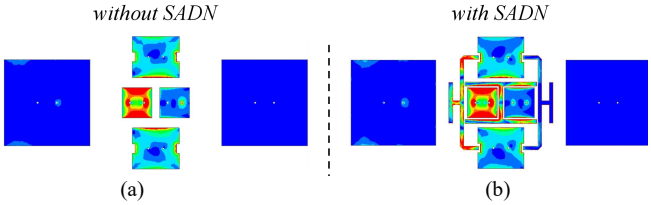

Figure 3. Current distributions of the tri-band DFA array (a) without and (b) with the SADN, when HB DFA 1 is excited at 28 GHz.

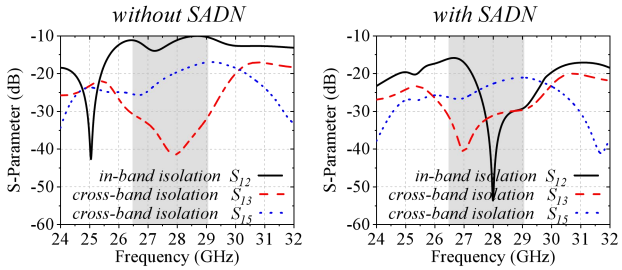

Figure 4. Comparison of the coupling coefficients (a) without and (b) with the SADN, when HB DFA 1 is excited.

A. High-Band (HB) Decoupling

The current distributions of tri-band DFA array without and with SADN at 28 GHz is compared in Fig. 3 when the HB DFA 1 is excited. It is observed that the current distributions appear quite similar in both cases, raising the question of whether the SADN effectively manages the couplings. Fig. 4 presents the S-parameter results, including both in-band and cross-band coupling coefficients, without and with the SADN. Note that the SADN has minimal impact on the impedance matching. The highlighted area indicates the measured impedance bandwidth, which spans from 26.54 GHz to 29.04 GHz. The following observations can be made.

1) In-band isolation between DFA1 and DFA2 (S_{12}): Significant improvement is achieved, increasing from 9 dB to over 50 dB around the center frequency.

2) Cross-band isolation between HB DFA1 and MB DFA3 (S_{13}): Results remain similar in both cases.

3) Cross-band isolation between HB DFA1 and LB DFA5 (S_{15}): Slight improvement is observed within the frequency range of 28 to 29 GHz.

The improvements in in-band isolation (S_{12}) and cross-band isolation (S_{15}) cannot be directly inferred from the current distribution shown in Fig. 3. Traditionally, decoupling is expected to minimize the currents induced on adjacent elements. However, in this work, decoupling is achieved using the SRCC method, which is uniquely designed for DFAs. As illustrated in Fig. 5, suppose the excited current on HB DFA1 is I_E and the induced current is I_C. Unlike the traditional decoupling principle, which aims to suppress the coupling current to zero, i.e., $I_{CP2+} = I_{CP2-} = 0$, the SADN retains the coupling currents but ensures they have equal amplitudes and phases at the two ports of coupled DFAs, i.e., $I_{CP2+} = I_{CP2-}$. These induced currents flowing into the differential power dividers can cancel each other, achieving isolation enhancement.

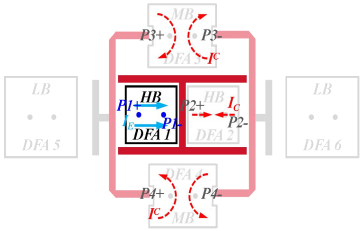

Figure 5. Decoupling current analysis of the tri-band DFA array with the SADN when HB DFA 1 is excited.

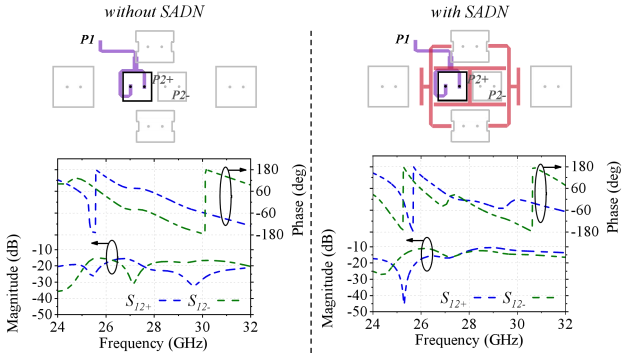

Figure 6. Illustration of feeding method of the array and the magnitudes and phases of S_{12+} and S_{12-} (a) without and (b) with the SADN.

To explore the quantitative aspects further, another simulation was performed, as shown in Figs. 6(a) and 6(b). In this setup, DFA1 was excited through one port (Port 1) after the power divider, while all other DFAs are individually fed through their respective two differential ports. For instance, DFA2 is fed through P2+ and P2-, allowing the magnitude and phase of the coupling currents at these ports to be monitored. As depicted in Fig. 6(a), without the SADN, there is a significant discrepancy between the magnitudes of S_{12+} and S_{12-}. Furthermore, the phase S_{12+} and S_{12-} are nearly out-of-phase, causing the coupling signals to add up after passing through the differential power divider. This results in poor isolation, with a value of only around 8 dB, as depicted in Fig. 4(a). However, as shown in Fig. 6(d), the SADN aligns the magnitude and phases of S_{12+} and S_{12-}, ensuring their consistency within the HB from 26.54 to 29.04 GHz. This effectively suppresses the coupling to less than -20 dB across the HB, with a remarkable isolation of 53 dB achieved at the center frequency.

Note that the cross-band isolation between HB DFA1 and MB DFA3 remains high without or with the SADN, which is also attributed to the SRCC principle. The S_{13+} and S_{13-} are consistent, allowing for high cross-band isolation S_{13} shown in Fig. 4(a). The results are omitted here for clarity. The slight improvement in isolation between HB DFA1 and LB DFA5 is attributed to a different mechanism. As shown in Fig. 3(b), a portion of the coupling energy is redirected to the bracket strips in the SADN, thereby reducing the coupled energy on DFA5.

B. Mid-Band (MB) and Low-Band (LB) Decoupling

Figs. 7(a) and 7(b) compare the current distributions of the DFA array without and with the SADN, respectively, at the center frequency of the MB when MB DFA3 is excited. The coupling coefficients in the two cases are compared in Figs. 8(a) and 8(b).

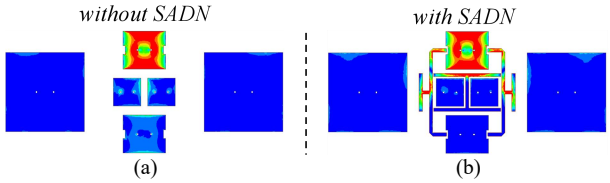

Figure 7. Current distributions of the tri-band DFA array (a) without and (b) with the SADN at 18.5 GHz when MB DFA3 is excited.

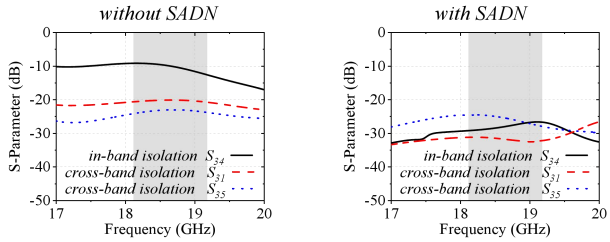

Figure 8. Comparison of the coupling coefficients (a) without and (b) with the SADN, when MB DFA 3 is excited.

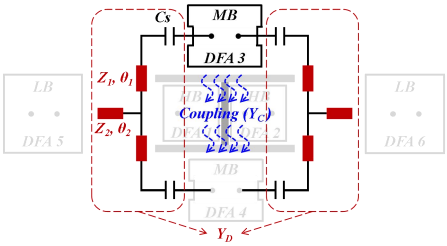

Figure 9. Equivalent circuit of the effective segments of SADN for addressing the in-band coupling between the two MB DFAs.

It is clear from Fig. 7 that the induced currents on the other MB DFA4 and two HB DFAs have been greatly suppressed after adding the SADN. This agrees with the significant isolation improvement in S_{34} and S_{31} as observed in Fig. 8. Suppressing the in-band coupling between the two MB DFAs and the cross-band coupling between the MB DFA and the HB DFA employs a different strategy, wherein the SADN is configured as a differential and symmetrical decoupling network, functioning as a pair of neutralization lines. The equivalent circuit of this decoupling network addressing the in-band coupling is illustrated in Fig. 9 as an example, with the detailed derivation process available in our previous work [4]. On the other hand, the couplings on the LB DFAs remain consistently low, regardless of the presence of the SADN.

Finally, when the LB DFA5 is excited, the induced currents on all the other DFAs remain very low, both without and with the SADN. Although the SADN does not further enhance isolation at the LB, it does not compromise the decoupling efficiency of the dual-band array. The in-band and cross-band couplings are consistently below -20 dB across the LB, as shown in Fig. 11 in the next section. These results are omitted here due to space constraints. This behavior is primarily attributed to the relatively larger separation distance between the LB DFAs and other DFAs, as well as the small size of the HB and MB DFAs at the LB frequency, which prevents significant current induction when an LB DFA is excited.

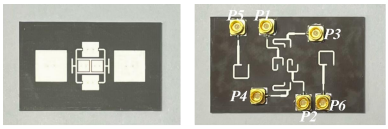

(a) (b)

Figure 10. (a) Top and (b) bottom view of the fabricated prototype.

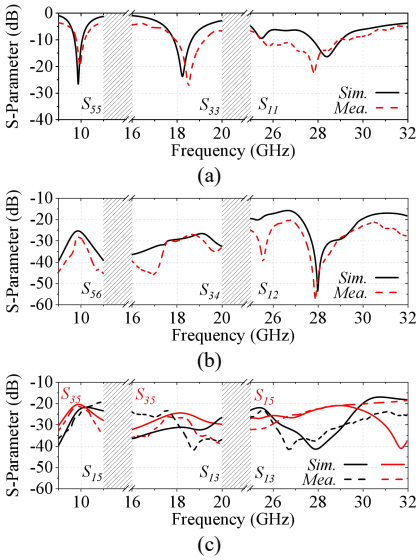

Figure 11. Simulated and measured (a) reflection coefficients, (b) in-band coupling coefficients, and (c) cross-band coupling coefficients of the tri-band DFA array.

III. Simulated and Experimental Results

The tri-band DFA array was also fabricated and tested. The prototype is shown in Fig. 10. Fig. 11(a) displays the simulated and measured reflection coefficients for LB, MB, and HB antennas. The array has measured reflection coefficients less than -10 dB across three bands: HB (25.5-28.94 GHz), MB (18.07-19.2 GHz), and LB (9.83-10.18 GHz), with bandwidths of 3.5%, 6.1%, and 12.5%, respectively. These bands include X-band and 5G NR (n257, n510-n512 downlink), supporting both terrestrial and non-terrestrial communications. Figs. 11(b) and 11(c) illustrate the in-band and cross-band coupling coefficients at the three bands. All couplings between any ports are below -20 dB across any one of the three bands and can reach as low as -52 dB. Fig. 12 compares the simulated and measured radiation patterns for DFAs 1, 3, and 5, showing close alignment. Measured gains for LB, MB, and HB DFAs are around 7.5 dBi, 6.8 dBi, and 6.1 dBi, respectively.

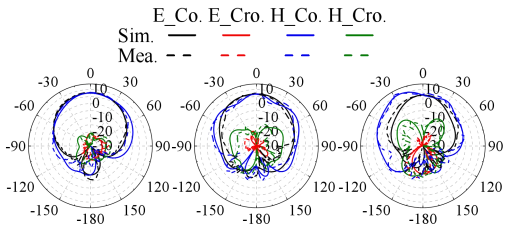

Figure 12. Simulated and measured E-plane and H-plane radiation patterns of (a) the LB DFA 5 at 10 GHz, (b) the MB DFA 3 at 18.5 GHz, and (c) the HB DFA 1 at 28 GHz in the tri-band DFA array.

The decoupling performance of the SADN for the tri-band array is compared with other works in Table I, highlighting its superior performance. No single decoupling structure has previously addressed multiple couplings in a tri-band array as effectively as this one. Most importantly, both the array and the SADN exhibit remarkable simplicity, attributed to the novel SRCC method and the aperture-sharing design.

IV. Conclusion

An all-in-one shared-aperture decoupling network (SADN) is proposed to manage the multiple coupling challenges within a tri-band DFA array. The SADN simultaneously addresses both in-band and cross-band couplings in multi-band shared-aperture DFA arrays. It employs distinct mechanisms at different frequency bands, each detailed through current distribution and S-parameter analyses.

References

[1] Y. Li and Q. -X. Chu, "Self-Decoupled Dual-Band Shared-Aperture Base Station Antenna Array," *IEEE Trans. Antennas Propag.*, vol. 70, no. 7, pp. 6024-6029, July 2022.

[2] H. Yuan, F. -C. Chen, W. -F. Zeng and Q. -X. Chu, "Dual-Band Base Station Antenna Array With Cross-Band Scattering and In-Band Coupling Suppression," *IEEE Trans. Antennas Propag.*, vol. 71, no. 5, pp. 3983-3991, May 2023.

[3] S. -Y. Sun, C. Ding, W. Jiang and Y. J. Guo, "Simultaneous Suppression of Cross-Band Scattering and Coupling Between Closely Spaced Dual-Band Dual-Polarized Antennas," *IEEE Trans. Antennas Propag.*, vol. 71, no. 8, pp. 6423-6434, Aug. 2023.

[4] X. Wang, C. Ding, G. Zhao, S. Li, Y. Chen and H. Sun, "Differential and Symmetrical Decoupling Network for Differentially-Fed Antennas," *IEEE Antennas Wireless Propag. Lett.*, vol. 23, no. 3, pp. 1129-1133, March 2024.

[5] J. Xu, X. He and T. Deng, "A Self-Decoupled MIMO Patch Array With Consistent Radiation Patterns," *IEEE Trans. Antennas Propag,* vol. 72, no. 12, pp. 8971-8979, Dec. 2024.

TABLE I. Comparison between state-of-the-art multi-band shared-aperture antenna arrays

Ref.	Method	f	ES	Profile	Bandwidth	Isolation		Isolation Improvement	
						within BW	at f	within BW	at f
[1]	Self-Decoupling	f_L: 1.9 GHz f_H: 3.5 GHz	0.7 λ_H	0.25 λ_L	LB: 15.6% HB: 7.7%	LB: NG HB: > 27 dB Cx: NG	LB: NG HB: 38.6 dB Cx: NG	LB: NG HB: 9 dB Cx: NG	LB: NG HB: 18 dB Cx: NG
[2]	Path Extension	f_L: 0.86 GHz f_M: 1.9 GHz f_H: 3.5 GHz	0.5 λ_L 0.35 λ_M 0.64 λ_H	0.13 λ_L	LB: 19.8% MB: 24.2% HB: 5.7%	LB: > 28 dB MB: > 25 dB HB: > 20 dB Cx: NG	LB: 30 dB MB: 30 dB HB: 26 dB Cx: NG	LB: 6 dB MB: NG HB: NG Cx: NG	LB: 10 dB MB: NG HB: NG Cx: NG
Our Work	**SADN**	**f_L: 10 GHz f_M: 18.5 GHz f_H: 28 GHz**	**0.7 λ_L 0.7 λ_M 0.07 λ_H**	**0.03 λ_L**	**LB: 3.7% MB: 7.1% HB: 12.5%**	**LB: > 28 dB MB: > 27 dB HB: >20 dB Cx: >22 dB**	**LB: 28 dB MB: 27 dB HB: 52 dB Cx: 24 dB**	**LB: 2 dB MB: 20 dB HB: 12 dB Cx: 6 dB**	**LB: 2 dB MB: 20 dB HB: 44 dB Cx: 10 dB**